Kinetic mechanism of adenine nucleotide binding to and hydrolysis by the Escherichia coli Rep monomer. 2. Application of a kinetic competition approach

ARTICLE *in* BIOCHEMISTRY · JANUARY 1995

Impact Factor: 3.02 · DOI: 10.1021/bi00252a024 · Source: PubMed

2 AUTHORS, INCLUDING:

Timothy M. Lohman
Washington University in St. Louis
189 PUBLICATIONS **12,037** CITATIONS

Kinetic Mechanism of Adenine Nucleotide Binding to and Hydrolysis by the *Escherichia coli* Rep Monomer. 2. Application of a Kinetic Competition Approach†

Keith J. M. Moore and Timothy M. Lohman*

Department of Biochemistry and Molecular Biophysics, Washington University School of Medicine, Box 8231, 660 South Euclid Avenue, St. Louis, Missouri 63110

Received July 15, 1994®

ABSTRACT: The *Escherichia coli* Rep protein is a DNA helicase that functions as a homodimer to catalyze the unwinding of duplex DNA during DNA replication in a reaction that is coupled to the binding and hydrolysis of ATP. As a first step toward a molecular understanding of the interactions of Rep with adenine nucleotides, we have investigated the kinetic mechanism of adenine nucleotide binding to the Rep monomer, which is the state of the protein in the absence of DNA. Although ATP binding to Rep does not significantly change the intrinsic tryptophan fluorescence, the binding of the fluorescent nucleotide analogue, 2′(3′)-*O*-(*N*-methylanthraniloyl)-ATP (mantATP) is associated with a large increase in mant nucleotide fluorescence intensity [λ_{ex} = 290 nm, λ_{em} > 420 nm; Moore, K. J. M., & Lohman, T. M. (1994) *Biochemistry* (preceding article in this issue)]. We have used the fluorescence signal from mantATP binding to monitor the kinetics of nonfluorescent nucleotide binding to Rep by a kinetic competition approach. The simultaneous and parallel binding of a mixture of mantATP and ATP to the Rep monomer is associated with a complex triphasic fluorescence transient during the approach to equilibrium. Global analysis of the fluorescence transients over a range of [ATP] by numerical integration techniques was used to define the kinetic mechanism of ATP binding and to determine the elementary rate constants. Using this approach, the kinetic rate constants for ADP, ATPγS, AMPPNP, AMP, adenosine, and inorganic phosphate were also determined at 4 °C in 20 mM Tris·HCl (pH 7.5), 6 mM NaCl, 10% (v/v) glycerol, and 5 mM $MgCl_2$. The kinetics of adenine nucleotide binding to the Rep monomer are similar to those observed with the mant nucleotides under identical experimental conditions (Moore & Lohman, 1994). The kinetic competition data are consistent with the following two-step mechanism for the binding of ATP, ADP, and ATPγS, where P is the Rep monomer and A is the adenine nucleotide: $P + A \underset{k_{-1}}{\overset{k_{+1}}{\leftrightarrow}} P{-}A \underset{k_{-2}}{\overset{k_{+2}}{\leftrightarrow}} (P - A)^*$. In the presence of 5 mM $MgCl_2$, the values of k_{+1} ($\sim 10^7$ M^{-1} s^{-1}) and k_{+2} (~ 10 s^{-1}) are comparable for each nucleotide, whereas $k_{+2} > k_{-1}$ for ATP and ATPγS while for ADP $k_{+2} \ll k_{-1}$; hence, differences in the overall equilibrium binding affinities of these nucleotides are primarily due to changes in k_{-1}. This reaction represents the *minimal* mechanism for the binding of ATP to Rep in the absence of Mg^{2+}, where the four rate constants are similar to those observed with mantATP under the same conditions. Kinetic competition experiments with imidoadenosine 5′-triphosphate (AMPPNP) indicate the presence of an additional slow step to form a third species, (P−A)**; thus, the binding kinetics of AMPPNP are qualitatively different from those of ATP. The slow apparent binding of AMPPNP to Rep is the consequence of a high value of k_{-1} rather than a low value of k_{+1}. In contrast, the kinetics of AMP and adenosine (Ado) binding can be described by a single-step mechanism. The overall apparent affinities of Rep for ATP, ADP, AMP, and Ado are $\sim 10^8$, 10^6, 10^4, and 10^2 M^{-1}, respectively. We have also examined the effects of a variety of salts on the kinetics of mantATP binding to the Rep monomer. The major effect of these salts is an *apparent* reduction in the association rate constant, k_{+1} [effects decrease in the order $(NH_4)_2SO_4 > Na_2SO_4 > NaP_i \gg NH_4Cl > NaCl$], whereas the unimolecular rate constants remain unchanged. Specific effects of both anions and cations are observed, reflecting direct binding of both anions and cations to the Rep monomer, although multivalent anions are most effective. These results are consistent with the competitive binding of anions to the ATP binding site of Rep. Qualitatively similar results are obtained with NaCl and NH_4Cl, although at significantly higher concentrations (20−50 mM), indicating a lower affinity of Rep for Cl^-, relative to phosphate and sulfate.

The ability of DNA helicases to catalyze the unwinding of duplex DNA is coupled to the binding and hydrolysis of nucleoside 5′-triphosphates [for reviews, see Matson and Kaiser-Rogers (1990), Matson (1991), and Lohman (1992, 1993)]. We have been using the *Escherichia coli* Rep helicase in order to investigate the mechanistic details of the DNA unwinding reaction, including the role of ATP binding and hydrolysis (Chao & Lohman, 1990, 1991; Wong et al., 1992; Wong & Lohman, 1992; Amaratunga & Lohman, 1993).

Although the Rep helicase appears to function as a dimer, dimerization is induced only upon binding DNA (Chao &

† This work was supported in part by grants to T.M.L. from the American Cancer Society (NP-756B) and the NIH (GM 45948). K.J.M.M. is the recipient of a William M. Keck Foundation Postdoctoral Fellowship.

* Address correspondence to this author at the Department of Biochemistry and Molecular Biophysics, Washington University School of Medicine, Box 8231, 660 South Euclid Ave., St. Louis, MO 63110. Telephone: (314)-362-4393. FAX: (314)-362-7183.

® Abstract published in *Advance ACS Abstracts,* November 1, 1994.

0006-2960/94/0433-14565$04.50/0

Scheme 1

$$P + \text{mantATP} \underset{k_{-1}}{\overset{k_{+1}}{\rightleftharpoons}} \text{P–mantATP} \underset{k_{-2}}{\overset{k_{+2}}{\rightleftharpoons}} (\text{P–mantATP})^*$$

Lohman, 1991; Wong et al., 1992; Wong & Lohman, 1992). Therefore, prior to initiating studies of the DNA-stimulated ATPase activities of the dimeric Rep helicase, we first investigated ATP binding and hydrolysis by the Rep monomer. In the accompanying paper (Moore & Lohman, 1994), we report studies of the kinetics and mechanism of Rep monomer binding to a series of fluorescent nucleotide analogues that have the *N*-methylanthraniloyl-ATP (mantATP[1]) fluorophore attached to the 2′- or 3′-hydroxyl group of the ribose moiety (Hiratsuka, 1983). The use of these analogues was necessary for kinetic studies since there is no significant change in the intrinsic protein fluorescence of the Rep monomer upon binding ATP or ADP. The results of these stopped-flow studies of mant nucleotide binding to the Rep monomer were consistent with a two-step mechanism (Scheme 1) involving the initial binding of mantATP to Rep monomer (P), followed by a conformational change in the P–mantATP complex to yield (P–mantATP)*. The four rate constants in Scheme 1, determined at 4 °C (pH 7.5, 6 mM NaCl, 5 mM $MgCl_2$, and 10% (v/v) glycerol), are $k_{+1} = 1.2 \times 10^7$ M^{-1} s^{-1}, $k_{-1} \sim k_{+2} \sim 3$ s^{-1}, and $k_{-2} = 0.04$ s^{-1}.

Fluorescently modified substrates have been widely used to probe the interaction of enzymes with their substrates, and mant nucleotides have been used extensively in the study of both ATPases and GTPases [see Moore and Lohman (1994), accompanying paper]. In general, mant nucleotides behave as good analogues of the parent nucleotides with a variety of ATPases and GTPases. In fact, mantATP can support Rep-catalyzed DNA unwinding and is hydrolyzed only ~2-fold slower than ATP. However, in certain cases a fluorescence modification of the nucleotide does alter the association and dissociation rate constants significantly [e.g., see Woodward et al. (1991), Geeves (1992), and Jackson and Bagshaw (1988a,b)].

We have therefore determined the kinetic mechanism and elementary rate constants for the binding of the nonfluorescent parent nucleotides (ATP, ADP, ATPγS, AMPPNP, AMP, etc.) to the Rep monomer in order to compare them with those determined for the mant derivatives (Moore & Lohman, 1994). This has been accomplished using a kinetic competition approach in which the binding and dissociation of ATP (or other nonfluorescent ligand) to Rep is determined indirectly from the effect of ATP on the kinetics of mantATP binding. This approach should prove generally useful for similar mechanistic studies of nucleotide binding to other helicases.

MATERIALS AND METHODS

The preparation and purification of *E. coli* Rep protein and the fluorescent mant nucleotides are described in the accompanying paper (Moore & Lohman, 1994). ATPγS (containing 5–10% ADP) was purchased from Sigma (St. Louis, MO) and repurified to >98% purity by DE-52 TEAB ion exchange chromatography with a 0.1–0.5 M TEAB gradient as described (Moore & Lohman, 1994) and used within 1 h of purification. Adenine nucleotide stock solutions were neutralized to pH 7.0 with NaOH and stored at −20 °C in H_2O. Stopped-flow experiments were performed at 4 °C in 20 mM TrisHCl (pH 7.5), 6 mM NaCl, 5 mM $MgCl_2$, and 10% (v/v) glycerol (buffer A) using an Applied Photophysics !SX17MV stopped-flow spectrophotometer (Applied Photophysics Ltd., Leatherhead, U.K.) as described (Moore & Lohman, 1994).

Kinetic simulations of reaction mechanisms were performed using either the program KSIM (from Dr. N. Millar, Kings College, London) or KINSIM (from Dr. C. Frieden, Washington University). Stopped-flow data were analyzed by numerical integration fitting routines using the PC versions of KINSIM and FITSIM (Barshop et al., 1983; Zimmerle et al., 1987; Zimmerle & Frieden, 1989). All simulation programs were run on an IBM 486 PC. A maximum of 16 different fluorescence transients could be fit simultaneously by FITSIM. Three different time domains were used to selectively monitor each of the three phases of the fluorescence changes that were observed (e.g., see Figure 1A). Unless stated otherwise, the data were fit globally to Scheme 2 (see Results). The observed fluorescence intensity $F_{obs} = X_1([\text{P–mantATP}] + [(\text{P–mantATP})^*])$, where X_1 is a constant determined from a reaction trace in the absence of competitor [analogous to Figure 2A in the accompanying paper (Moore & Lohman, 1994)]. Under these conditions Rep (0.2 μM) is saturated with mantATP at the end of the fluorescence transient and $X_1 = (\Delta F_{obs}/0.2)\ \mu\text{M}^{-1}$. The same value of X_1 was used for all of the traces within a given experiment. Fitting of the data was achieved in three steps: (1) approximate estimations were obtained for those rate and equilibrium constants that can be determined independently by conventional fitting (e.g., $k_{+1,M}$ and $k_{+1,A}$) and from estimates of the rate constants for mantATP binding alone [see Moore and Lohman (1994)]; (2) visual refinement of the fit to the data by the simulation program KINSIM was then used to provide estimates of the other rate constants; and (3) global fitting of the data using FITSIM to obtain a unique determination of all of the rate constants in the mechanism. In all cases, attempts were made to fit the experimental data to mechanisms of either greater or lesser complexity than that shown in Scheme 2. The appropriate mechanism was determined to be the one that required the minimum number of steps to describe the data both qualitatively and quantitatively. The estimates of the variability in the resolved values of elementary rate constants that we report are based on analyses of different samples of the entire data set (only five competitor concentrations over three time domains could be analyzed simultaneously).

RESULTS

In the accompanying paper (Moore & Lohman, 1994), we report studies of the kinetics and mechanism of Rep monomer binding to a series of fluorescently labeled (mant) nucleotides, which undergo a substantial increase in fluorescence intensity upon binding Rep due to energy transfer

[1] Abbreviations: mantATP, 2′(3′)-*O*-(*N*-methylanthraniloyl)adenosine 5′-triphosphate; 3′-mant-dATP, 3′-*O*-(*N*-methylanthraniloyl)-2′-deoxyadenosine 5′-triphosphate; other mant nucleotides and mant deoxyribonucleotides are abbreviated similarly; AMPPNP, imidoadenosine 5′-triphosphate; ATPγS, adenosine 5′-thiotriphosphate; Ado, adenosine; EDTA, ethylenediamine-*N*,*N*,*N*′,*N*′-tetraacetic acid; TEAB, triethylammonium bicarbonate; HPLC, high-performance liquid chromatography; TLC, thin-layer chromatography.

Scheme 2

$$P + \text{mantATP} \underset{k_{-1,M}}{\overset{k_{+1,M}}{\rightleftharpoons}} \text{P–mantATP} \underset{k_{-2,M}}{\overset{k_{+2,M}}{\rightleftharpoons}} (\text{P–mantATP})^*$$

$$P + \text{ATP} \underset{k_{-1,A}}{\overset{k_{+1,A}}{\rightleftharpoons}} \text{P–ATP} \underset{k_{-2,A}}{\overset{k_{+2,A}}{\rightleftharpoons}} (\text{P–ATP})^*$$

from Rep tryptophans. In this paper we use a kinetic competition approach in which the binding and dissociation of ATP (and other nonfluorescent ligands) are monitored indirectly through their effect on the kinetics of mantATP binding to Rep. The analysis of the data is based on the kinetics of parallel reactions, since in these experiments a premixed solution of mantATP and ATP is subsequently mixed with the Rep monomer in stopped-flow conditions so that the two nucleotides can bind to Rep simultaneously and in parallel. The time course of the approach to equilibrium is monitored at a fixed [mantATP] and several [ATP]; in favorable circumstances, the time dependence of the fluorescence changes can then be used to determine the kinetic mechanism for the binding of the unlabeled ligand (e.g., ATP).

ATP Binding to the Rep Monomer Monitored by Kinetic Competition with mantATP. When a solution of mantATP (3 μM) plus ATP (1−30 μM) was rapidly mixed with Rep monomer (0.2 μM), the subsequent fluorescence change was composed of three discrete phases, each of which could be described by a single-exponential function. Figure 1A shows representative fluorescence transients at five [ATP] plotted on a logarithmic time scale. *A priori*, the observation of three exponential phases indicates a *minimum* of three kinetically significant species in the binding mechanism and requires the binding of *at least* one of the nucleotides to be a two-step process. Each phase of the reaction is sensitive to, and provides information to determine, the different rate constants. For example, the first phase monitors the initial binding step, while the third slow phase represents the approach to final thermodynamic equilibrium.

To interpret these data, we consider a model in which ATP binding occurs by a two-step reaction analogous to that shown in Scheme 1 for mantATP. Scheme 2 shows the chemical equations relevant to the analysis of Figure 1 based on this model. The subscripts M and A in Scheme 2 distinguish the rate constants for the mant nucleotides from those for the parent adenine nucleotides. Since there is no analytical solution to the rate equations for the mechanism shown in Scheme 2, in the absence of certain assumptions that are invalid in this system, a quantitative analysis of the data requires the use of numerical integration techniques (e.g., FITSIM, see below). We initially consider each phase of the fluorescence change in isolation to provide a qualitative description of the kinetic origins of the observed fluorescence changes and to obtain estimates of the rate constants to be used as initial guesses in the FITSIM analysis. However, we emphasize that the assumptions and approximations that are inherent in the following discussion are unnecessary and are not used in the FITSIM analysis.

Phase I. The fast phase of the fluorescence change is primarily dependent on the bimolecular association rate constants ($k_{+1,A}$ and $k_{+1,M}$). For a fixed [mantATP] and increasing [ATP], Figure 1B shows that the exponential rate constant of the rapid increase in fluorescence, $k_{obs,1}$, increases linearly with [ATP], while its amplitude decreases hyperbolically. When [nucleotide] ≫ [Rep] and $k_{-1,M}$ and $k_{-1,A}$ are

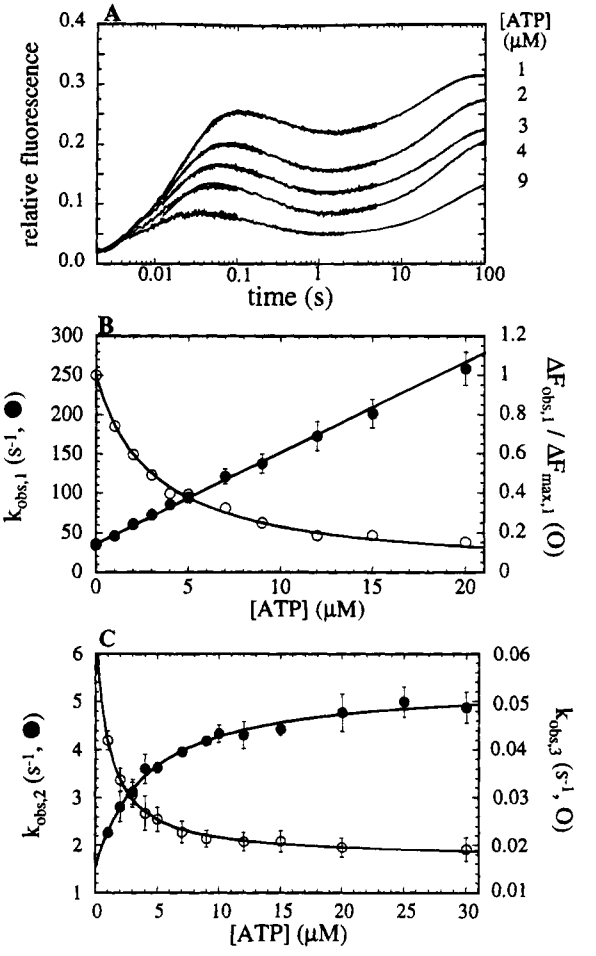

FIGURE 1: Kinetics of ATP binding to Rep determined by kinetic competition with mantATP. (A) Rep monomer (0.2 μM) in buffer A at 4 °C was mixed in a stopped-flow experiment with a solution of mantATP (3 μM) in buffer A containing ATP (1−20 μM), and the change in mant fluorescence (λ_{ex} = 290 nm, λ_{em} > 420 nm) for experiments at five concentrations of ATP is shown as a function of time (note the logarithmic scale). Three exponential phases of the fluorescence change are characterized by observed rate constants, $k_{obs,1}$, $k_{obs,2}$, and $k_{obs,3}$. (B) Dependence of $k_{obs,1}$ (●) and $\Delta F_{obs,1}$ (○) on [ATP]. The solid lines represent the best fits of $k_{obs,1}$ to eq 1 and of $\Delta F_{obs,1}$ to eq 2, yielding $k_{+1,A}$ = (1.16 ± 0.03) × 10^7 and (1.19 ± 0.040 × 10^7 M^{-1} s^{-1}, respectively ($k_{+1,M}$ = 1.2 × 10^7 M^{-1} s^{-1} in eq 2). (C) Dependence of $k_{obs,2}$ and $k_{obs,3}$ on [ATP]. The solid lines are best fits of the data to a simple hyperbola. (○) $k_{obs,2}$: intercept = 1.5 (±0.2) s^{-1}, plateau = 5.0 (±0.2) s^{-1}, K_{app} = 0.26 (±0.04) μM^{-1}. (●) $k_{obs,3}$: intercept = 0.067 (±0.010) s^{-1}, plateau = 0.018 (±0.003) s^{-1}, K_{app} = 1.0 (±0.2) μM^{-1}.

small compared to $k_{+1,M}$[mantATP] and $k_{+1,A}$[ATP], respectively, then $k_{obs,1}$ and $\Delta F_{obs,1}$ vary with [ATP] according to eqs 1 and 2 (Eccleston & Trentham, 1979; Novak & Goody, 1988):

$$k_{obs,1} = k_{+1,M}[\text{mantATP}] + k_{-1,M} + k_{+1,A}[\text{ATP}] + k_{-1,A} \quad (1)$$

$$\Delta F_{obs,1}/\Delta F_{max,1} = 1/[1 + (k_{+1,A}[\text{ATP}]/k_{+1,M}[\text{mantATP}])] \quad (2)$$

Since $k_{+1,M}$ = 1.2 × 10^7 M^{-1} s^{-1} (Moore & Lohman, 1994), we estimate $k_{+1,A}$ = (1.2 ± 0.05) × 10^7 M^{-1} s^{-1} from the dependence of either $k_{obs,1}$ or $\Delta F_{obs,1}$ on [ATP] (Figure 1B). Thus, the association rate constants for ATP and mantATP are essentially identical (i.e., $k_{+1,M}$ = $k_{+1,A}$).

Phase II. The second phase of the fluorescence transient is associated with a small decrease in fluorescence intensity occurring from ~0.1 to 2 s. During phase II, the species distribution changes in a complex manner (see Figure 2B), where the observed rate constant and amplitude of the process are dependent on the values of several rate constants in the mechanism. This phase represents the transformation of the initial species distribution (dictated primarily by $k_{+1,M}$[mantATP] *vs* $k_{+1,A}$[ATP]) to a quasi-equilibrium state. The species distribution that exists at the end of this phase is governed by the kinetic partitioning of the initial collisional complexes (P−mantATP and P−ATP) to dissociate ($k_{-1,M}$, $k_{-1,A}$) or proceed in the forward direction ($k_{+2,M}$, $k_{+2,A}$). Intuitively, a decrease in fluorescence will be observed when $k_{-1,M} > k_{-1,A}$ and/or $k_{+2,M} < k_{+2,A}$, since both of these situations result in a net reduction in the concentration of protein-bound mantATP.

The observed rate constant, $k_{obs,2}$, increases from the limiting value of ~1.5 s^{-1} as [ATP] → 0, reaching a plateau at ~5 s^{-1} at high [ATP] (Figure 1C). In certain mechanisms, the limiting values of $k_{obs,2}$ determined at low and high [ATP] can be used to determine particular rate constants in the mechanism [see Novak and Goody (1988) and John et al. (1990)]. However, in these experiments, there is no simple relationship between the limiting values of $k_{obs,2}$ and the elementary rate constants in Scheme 2.

Phase III. During phase III, the nonequilibrium mixture of (P−mantATP)* and (P−ATP)* formed during phase II decays to thermodynamic equilibrium. The observed rate constant, $k_{obs,3}$, varies hyperbolically from a value equal to $k_{off,A}$ ($=k_{-1,A}k_{-2,A}/k_{-1,A} + k_{-2,A} + k_{+2,A}$) at low [ATP] to $k_{off,M}$ ($=k_{-1,M}k_{-2,M}/k_{-1,M} + k_{-2,M} + k_{+2,M}$) at high [ATP]. The limiting values of $k_{obs,3}$ determined from Figure 1C are consistent with those determined directly from cold chase displacement experiments [see Figure 4B of Moore and Lohman (1994), accompanying paper] using preformed Rep−mantATP and Rep−ATP complexes [0.021 (±0.002) s^{-1} and 0.067 (±0.004) s^{-1} respectively].

The end point (equilibrium) fluorescence intensity decreases with increasing [ATP] (Figure 2A) as expected for competitive binding of ATP and can be used to determine an apparent equilibrium constant for ATP, $K_{app,ATP}$ = 0.18 (±0.01) μM^{-1}. From eq 3 and a knowledge of $K_{mantATP} = K_{1,M}(1 + K_{2,M}) \sim 200\ \mu M^{-1}$ (Moore & Lohman, 1994), the true overall equilibrium association constant for ATP, $K_{ATP} = K_{1,A}(1 + K_{2,A})$, was calculated to be 110 (±5) μM^{-1}.

$$K_{ATP} = K_{app,ATP}(1 + K_{mantATP}[mantATP]) \quad (3)$$

Analysis of Kinetic Competition Experiments by Numerical Integration Techniques (FITSIM). The advantages (and for the experiments discussed here, the necessity) of analyzing data such as that shown in Figure 1A by numerical integration techniques rather than by analytical approximations have been discussed [see Barshop et al. (1983) and Johnson (1992)]. The amplitudes of the fluorescence transients are particularly sensitive to the rate constants in this mechanism, and therefore an additional constraint is imposed by directly fitting the complete experimental time courses. The values of the four rate constants describing the interaction of Rep monomer with ATP determined from a FITSIM analysis are given in Table 1. The predicted time-dependent distribution of the five Rep species shown in Scheme 2 based on these rate constants is shown in Figure 2B for the competitive binding of ATP (3 μM) and mantATP (3 μM) to Rep monomer (0.2 μM). The superposition of the predicted and observed transients over the entire time course of the reaction demonstrates that this model provides an excellent description of the data; similar quality fits are obtained at other [ATP].

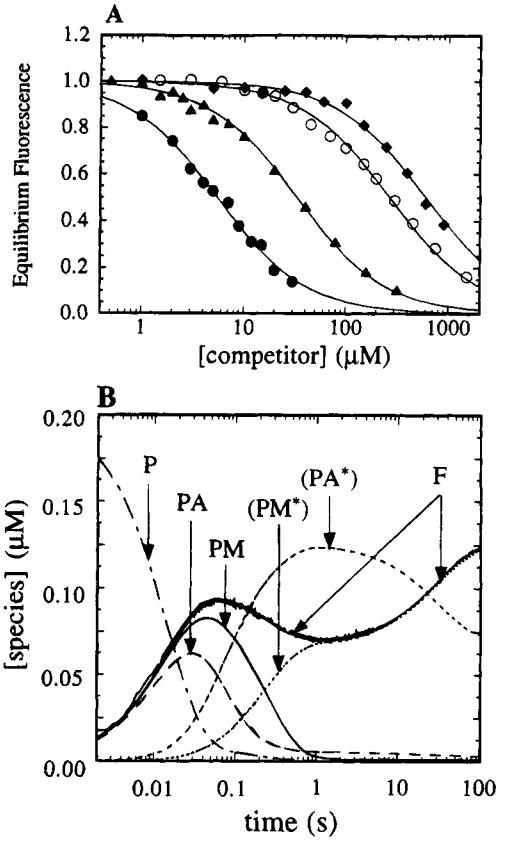

FIGURE 2: (A) Dependence of the end point (equilibrium) mantATP fluorescence intensity on the concentration of competitor nucleotide. The equilibrium fluorescence intensity in the absence of competitor was 1. All experiments used 0.2 μM Rep monomer and 3 μM mantATP, except for AMPPNP where [mantATP] = 1.8 μM: (●) ATP; (▲) ATPγS; (○) AMPPNP; (◆) ADP. The solid lines are best fits of the data to eq 3, with K_{ATP} = 110 (±5) μM^{-1}, $K_{ATP\gamma S}$ = 20 (±1) μM^{-1}, K_{AMPPNP} = 1.4 (±0.1) μM^{-1}, and K_{ADP} = 1.0 (±0.1) μM^{-1}. (B) KINSIM simulation of the time dependence of the species distribution in a kinetic competition experiment based on Scheme 2 (note the logarithmic time scale). The simulation was for 3 μM total mantATP, 3 μM total ATP, and 0.2 μM Rep monomer and is based on the rate constants for ATP shown in Table 1 and $k_{+1,M} = 1.2 \times 10^7\ M^{-1}\ s^{-1}$, $k_{-1,M}$ = 3.1 s^{-1}, $k_{+2,M}$ = 2.8 s^{-1}, and $k_{-2,M}$ = 0.036 s^{-1} for mantATP. Species are, from left to right, the Rep monomer (P), P−ATP, P−mantATP, (P−mantATP)*, (P−ATP)*, and (P−mantATP + (P−mantATP)*). Superimposed over curve 6 is the experimentally observed fluorescence trace, F_{obs}.

The rate constants for ATP binding and dissociation are comparable to those determined with mantATP and confirm that the initial binding step is not a rapid equilibrium for either nucleotide: $k_{-1,M} \sim k_{+2,M}$ for mantATP, while $k_{-1,A} < k_{+2,A}$ for ATP. Therefore, the fluorescence modification of ATP reduces the values of both the forward and reverse rate constants for the second step. Since $k_{+2,A} \gg k_{-1,A}$ for ATP binding under these conditions (i.e., in the presence of 5 mM Mg^{2+}), the data are relatively insensitive to the absolute value of $k_{-1,A}$, and the uncertainty in this rate constant is reflected in the errors associated with $k_{+2,A}$ and $k_{-2,A}$ (see Table 1). However, FITSIM reported essentially

Table 1: Kinetic and Equilibrium Constants for the Interaction of the Rep Monomer with Adenine Nucleotides at 4 °C[a]

$$P + A \underset{k_{-1,A}}{\overset{k_{+1,A}}{\leftrightarrow}} P{-}A \underset{k_{-2,A}}{\overset{k_{+2,A}}{\leftrightarrow}} (PA)^*$$

nucleotide	$k_{+1,A}$ (μM^{-1} s^{-1})	$k_{-1,A}$ (s^{-1})	$K_{1,A}$ (μM^{-1})	$k_{+2,A}$ (s^{-1})	$k_{-2,A}$ (s^{-1})	$K_{2,A}$	k_{off}[c] (s^{-1})	$K_{overall}$ (μM^{-1})	$K_{a,app}$[d] (calcd) (μM^{-1})	$K_{a,app}$[e] (obs) (μM^{-1})
ATP ($+Mg^{2+}$)	12 (±0.5)	[1.5][f]	[8]	[15]	[0.9]	[16]	0.067 (±0.002)	[128]	[136]	110 (±5)
ATP ($-Mg^{2+}$)[b]	≈90	440 (±30)	≈0.2	≈10	28 (±2)	≈0.4	28 (±2)	≈0.08	≈0.28	0.27 (±0.03)
ATPγS	15 (±0.5)	1.5 (±0.5)	10 (±3.3)	13 (±2)	8.6 (±1.5)	1.5 (±0.3)	0.60 (±0.02)	15 (±5)	25 (±6)	21 (±1)
ADP	6.7 (±0.9)	720 (±65)	0.0093 (±0.0016)	8.1 (±1.2)	0.067 (±0.002)	121 (±19)	0.067 (±0.002)	1.1 (±0.2)	1.1 (±0.2)	1.0 (±0.1)
AMP	6.9 (±0.3)	680 (±30)	0.0099 (±0.0004)				700 (±100)	0.0099 (±0.0004)		

[a] Conditions: 20 mM Tris·HCl (pH 7.5 at 4 °C), 6 mM NaCl, 5 mM $MgCl_2$, and 10% (v/v) glycerol (buffer A). [b] Conditions: 20 mM Tris·HCl (pH 7.5 at 4 °C), 6 mM NaCl, 2 mM EDTA, and 10% (v/v) glycerol (buffer AE). [c] $k_{off} = k_{obs}$ for nucleotide dissociation from a Rep−nucleotide complex. $K_{overall} = K_1K_2$. [d] Apparent overall affinity $= K_1 + K_1K_2$. calculated from the rate constants. [e] K_{app} was determined from Figure 2A. [f] Data in square brackets are subject to large (≈100%) error, as discussed in the text.

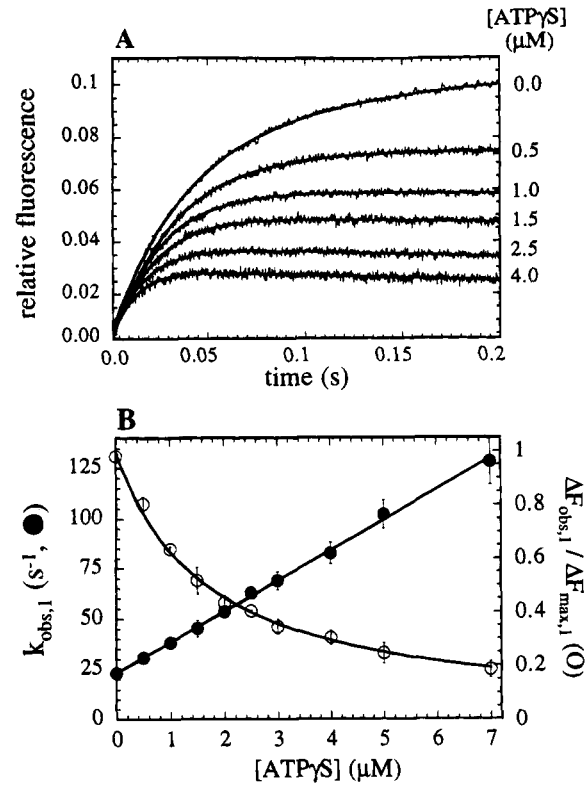

FIGURE 3: Binding of ATPγS to the Rep monomer in competition with mantATP. (A) Rep monomer (0.2 μM) in buffer A at 4 °C was mixed in a stopped-flow apparatus with a solution of mantATP (2 μM) containing ATPγS (0−320 μM). Fluorescence transients from experiments at five representative [ATPγS] are shown. (B) Dependence of $k_{obs,1}$ (●) and $\Delta F_{obs,1}$ (○) on [ATPγS] from experiments such as those shown in A. The data were fit to eqs 1 and 2 as in Figure 1, yielding $k_{+1,A} = (1.5 \pm 0.1) \times 10^7$ and $(1.4 \pm 0.1) \times 10^7$ M^{-1} s^{-1} from $k_{obs,1}$ and $\Delta F_{obs,1}$, respectively.

the same values for all four rate constants from different data sets. A consequence of $k_{+2,A}$ being significantly greater than $k_{-1,A}$ is that the two-step binding mechanism for ATP shown in Scheme 2 is difficult to distinguish unambiguously from a one-step binding mechanism. We nevertheless prefer Scheme 2 by analogy with the mechanism for mant nucleotide (Moore & Lohman, 1994) and ADP binding and on the basis of the results of kinetic competition experiments performed with ATP in the absence of Mg^{2+} (see below).

Binding of ATPγS to the Rep Monomer. The three phases of the fluorescence transient observed in a kinetic competition experiment with mantATP and ATPγS are qualitatively similar to those described above for ATP. The effect of increasing [ATPγS] on the kinetics of the initial mantATP binding transient is shown in Figure 3A. Direct fitting to eqs 1 and 2 of the dependence of either $k_{obs,1}$ or $\Delta F_{obs,1}/\Delta F_{max,1}$ on [ATPγS] (see Figure 3B) yields $k_{+1,A} = (1.5 \pm 0.1) \times 10^7$ M^{-1} s^{-1} for the association rate constant for ATPγS, which is slightly larger than the value determined for ATP binding. Interestingly, a similar slight increase in the association rate constant upon thiosubstitution was also observed with mantATPγS (Moore & Lohman, 1994). The dependence of $k_{obs,2}$ and $k_{obs,3}$ on [ATPγS] was similar to that observed with ATP, except that $k_{obs,3}$ approaches 0.62 (±0.02) s^{-1} at low [ATPγS]. The overall equilibrium association constant for ATPγS binding to Rep monomer determined from Figure 2A and eq 3 is 20 (±1) μM^{-1}, which is 5-fold lower than that for ATP. A FITSIM analysis of

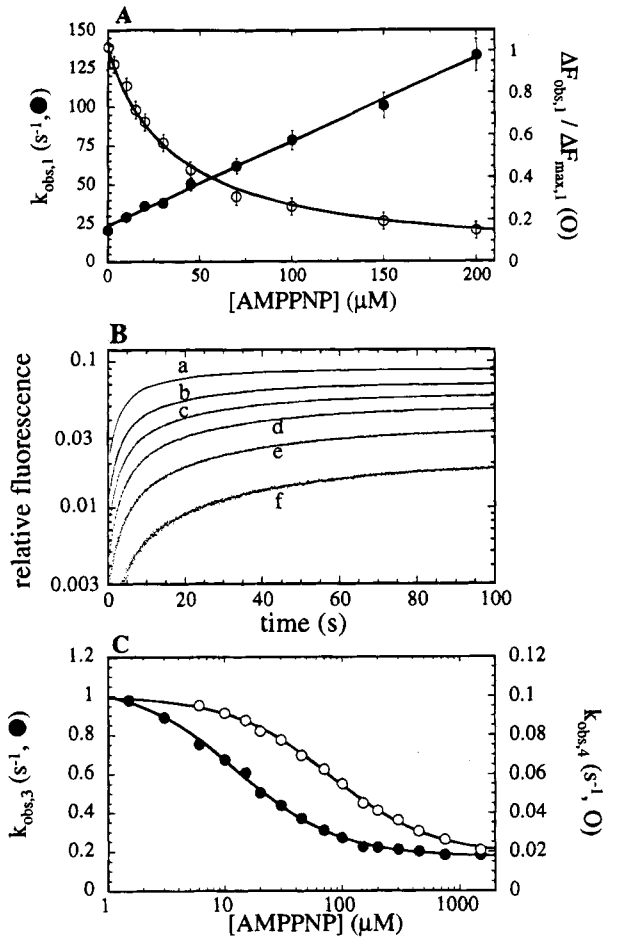

FIGURE 4: Binding of AMPPNP to the Rep monomer in competition with mantATP. (A) Dependence of $k_{obs,1}$ (●) and $\Delta F_{obs,1}$ (○) on [AMPPNP] from experiments analogous to those shown in Figure 1, but with 1.8 μM mantATP. The data were fit to eqs 1 and 2 as in Figure 1, yielding $k_{+1,A} = (5.4 \pm 0.2) \times 10^5$ and $(5.3 \pm 0.2) \times 10^5$ M^{-1} s^{-1} from $k_{obs,1}$ and $\Delta F_{obs,1}$, respectively. (B) The biphasic fluorescence change observed with six [AMPPNP] during the approach to equilibrium is plotted on a logarithmic scale as a function of time. Curves a–f were obtained at 100, 200, 300, 450, 750, and 1500 μM AMPPNP, respectively. (C) Each curve in B was fit to the sum of two exponentials defining observed rate constants $k_{obs,3}$ and $k_{obs,4}$; dependence of $k_{obs,3}$ and $k_{obs,4}$ on [AMPPNP] from experiments such as those shown in B. The solid lines are best fits of the data to hyperbolae. (●) $k_{obs,3}$: intercept = 1.0 ($\pm$0.1) s^{-1}, plateau = 0.17 ($\pm$0.05) s^{-1}, $K_{app} = (7.9 \pm 0.3) \times 10^4$ M^{-1}. (○) $k_{obs,4}$: intercept = 0.11 ($\pm$0.01) s^{-1}, plateau = 0.019 ($\pm$0.001) s^{-1}, $K_{app} = (1.25 \pm 0.05) \times 10^4$ M^{-1}.

the entire data set to Scheme 2 yields the rate constants in Table 1. The major difference between ATPγS and ATP (or their mant derivatives) is that the reverse rate constant for the second step ($k_{-2,A}$) is 10-fold larger for the thio nucleotide.

Binding of AMPPNP to the Rep Monomer. The kinetics of AMPPNP binding to Rep differs both qualitatively and quantitatively from that observed with ATP and ATPγS. Firstly, the apparent association rate constant determined from the dependencies of $k_{obs,1}$ and $\Delta F_{obs,1}$ on [AMPPNP] (Figure 4A) is $(5.4 \pm 0.2) \times 10^5$ M^{-1} s^{-1}, which is ~20-fold lower than that observed for ATP. $k_{obs,2}$ reached a plateau of 4.5 ($\pm$0.2) s^{-1} at high [AMPPNP], but could not be determined with sufficient accuracy below ~20 μM AMPPNP to fully define the concentration dependence of this process. Secondly, above 5 μM AMPPNP, the fluorescence transient was composed of *four* distinct phases. This

Scheme 3

$$\text{P + mantATP} \underset{k_{-1,M}}{\overset{k_{+1,M}}{\rightleftharpoons}} \text{P–mantATP} \underset{k_{-2,M}}{\overset{k_{+2,M}}{\rightleftharpoons}} \text{(P–mantATP)}^*$$

$$\text{P + AMPPNP} \underset{k_{-1,A}}{\overset{k_{+1,A}}{\rightleftharpoons}} \text{P–AMPPNP} \underset{k_{-2,A}}{\overset{k_{+2,A}}{\rightleftharpoons}}$$

$$\text{(P–AMPPNP)}^* \underset{k_{-3,A}}{\overset{k_{+3,A}}{\rightleftharpoons}} \text{(P–AMPPNP)}^{**}$$

difference is demonstrated most clearly in Figure 4B, which shows clear biphasic character up to the final increase in fluorescence intensity, whereas ATP and ATPγS show a single-exponential phase in this time range. The observed rate constants for the third and fourth phases, $k_{obs,3}$ and $k_{obs,4}$, decrease in a hyperbolic manner with increasing [AMPPNP], as shown in Figure 4C, while the relative contribution of ΔF_4 to the total biphasic fluorescence change ($\Delta F_3 + \Delta F_4$) increased over this concentration range (see the following). Finally, the overall equilibrium constant for AMPPNP binding to the Rep monomer is 1.4 ($\pm$0.1) μM^{-1} (Figure 2A), which is ~75-fold lower than that for ATP.

The observation of four phases for the fluorescence change suggests the presence of an additional step in the AMPPNP binding mechanism that is either not present or not observed for the binding of ATP and ATPγS. As a result, Scheme 3 is required to analyze the kinetic competition experiments with AMPPNP. Direct fitting of the data set to Scheme 3 using FITSIM yields the rate constants shown in Table 2. Scheme 3 provided a good fit to the data over the entire time course and range of concentrations used. The formation of the first kinetically stable Rep–AMPPNP complex occurs in two steps. The association rate constant for the first step ($k_{+1,A} = (1.0 \pm 0.02) \times 10^7$ M^{-1} s^{-1}) is essentially identical to that observed with ATP; however, initial binding is weak ($K_{1,A} = 0.014$ ($\pm$0.001) μM^{-1}) and rapidly reversible [$k_{-1,A} = 730$ ($\pm$75) s^{-1}]. The subsequent conformational change in the collisional complex (step 2 in Scheme 3) leads to the formation of the first tightly bound intermediate (P–AMPPNP)*, which yields an *apparent* association rate constant of $K_{1,A}k_{+2,A} = 5 \times 10^5$ M^{-1} s^{-1} (Figure 4A). The values of $K_{1,A}$, $k_{+2,A}$, and $k_{-2,A}$ are essentially identical to those determined for mantAMPPNP (Moore & Lohman, 1994), suggesting that the initial binding of mantAMPPNP is also a rapid equilibrium. The net dissociation of AMPPNP from the (P–AMPPNP)* complex allows subsequent binding of mantATP and gives rise to the third phase of the fluorescence change.

The dissociation of mantAMPPNP from a preequilibrated mixture of Rep and mantAMPPNP is biphasic ($k_{obs,1} \sim 0.6$ s^{-1}, $k_{obs,2} \sim 0.05$ s^{-1}; Moore & Lohman, 1994), suggesting the presence of two tightly bound Rep–mantAMPPNP complexes at equilibrium. These species are likely to be equivalent to (P–AMPPNP)* and (P–AMPPNP)** in Scheme 3 and suggest that the binding of mantAMPPNP may also be a three-step reaction. The data in Figure 4B provide direct evidence for the presence of this additional step with AMPPNP, although since $K_{3,A} < 1$, the additional conformational change does not lead to a marked increase in the overall affinity of Rep for AMPPNP. The exchange of AMPPNP for mantATP during the approach to equilibrium requires net dissociation of AMPPNP from this tight complex ((P–AMPPNP)**) and gives rise to the fourth phase of the fluorescence change in Figure 4B.

Table 2: Rate and Equilibrium Constants for the Interaction of the Rep Monomer with AMPPNP[a] (4 °C)

$$\mathrm{P} + \mathrm{A} \underset{k_{-1,\mathrm{A}}}{\overset{k^{+1,\mathrm{A}}}{\leftrightarrow}} \mathrm{P{-}A} \underset{k_{-2,\mathrm{A}}}{\overset{k_{+2,\mathrm{A}}}{\leftrightarrow}} (\mathrm{PA})^{*} \underset{k_{-3,\mathrm{A}}}{\overset{k_{+3,\mathrm{A}}}{\leftrightarrow}} (\mathrm{PA})^{**}$$

nucleotide	$k_{+1,A}$ (μM^{-1} s^{-1})	$k_{-1,A}$ (s^{-1})	$K_{a,A}$ (μM^{-1})	$k_{+2,A}$ (s^{-1})	$k_{2,A}$ (s^{-1})	$K_{2,A}$	$k_{+3,A}$ (s^{-1})	$k_{-3,A}$ (s^{-1})	$K_{3,A}$	$K_{overall}$[b] (μM^{-1})	$K_{a,app}$[c] (calcd) (μM^{-1})	$K_{a,app}$[d] (obs) (μM^{-1})
AMPPNP	9.9 (±0.2)	730 (±75)	0.014 (±0.001)	42 (±5)	0.73 (±0.08)	58 (±9)	0.036 (±0.003)	0.042 (±0.003)	0.86 (±0.09)	0.67 (±0.13)	1.5 (±0.3)	1.4 (±0.1)

[a] Conditions: 20 mM TrisHCl (pH 7.5 at 4 °C), 6 mM NaCl, 5 mM $MgCl_2$, and 10% (v/v) glycerol (buffer A). [b] $K_{overall} = K_1K_2K_3$. [c] Apparent overall affinity $= K_1(1 + K_2 + K_2K_3)$ calculated from the estimated rate constants. [d] Overall apparent affinity was determined from the equilibrium fluorescence intensity in Figure 2A.

Qualitatively, the data in Figure 4B,C can be rationalized as follows. The (P−AMPPNP)* complex can partition either forward (with apparent rate constant $k_{forward}$) to form (P−AMPPNP)** or backward (with rate constant $k_{reverse}$) to ultimately yield nucleotide-free Rep. At low [AMPPNP] (<5 μM), $k_{forward} \ll k_{reverse}$, such that $k_{obs,3} \sim k_{2,A}$ and an approximately single-exponential decay is observed ($\Delta F_3 \gg \Delta F_4$). However, as the [AMPPNP] is increased, $k_{reverse}$ decreases such that the (P−AMPPNP)* complex partitions more favorably in the forward direction and $k_{obs,3}$ decreases hyperbolically. The approach to thermodynamic equilibrium then involves dissociation from both (P−AMPPNP)* ($k_{obs,3}$) and (P−AMPPNP)** ($k_{obs,4}$), giving rise to a biphasic fluorescence change ($\Delta F_3 \sim \Delta F_4$). As the [AMPPNP] is increased further, $k_{obs,4}$ decreases and approaches $k_{off,mantATP}$, while ΔF_4 becomes $\gg \Delta F_3$.

Binding of ADP to the Rep Monomer. The parallel binding of a mixture of mantATP and ADP to Rep yields triphasic fluorescence kinetics (Figure 5A) similar to those observed with ATP and ATPγS. However, with ADP, both the amplitude ($\Delta F_{obs,1}$) and the observed rate constant of the fast phase ($k_{obs,1}$) *decrease* with increasing [ADP] (Figure 5B), such that $k_{obs,1}$ reaches a plateau of 13.6 (±0.5) s^{-1} at high [ADP]. $k_{obs,2}$ increases hyperbolically from ~1 to ~3.7 s^{-1} at high [ADP], while $k_{obs,3}$ decreases from 0.07 (±0.01) to 0.02 (±0.002) s^{-1} over the concentration range studied (data not shown). The apparent overall equilibrium constant for ADP binding was determined from Figure 2A and eq 3 to be 1.0 (±0.1) μM^{-1}. The *decrease* in $k_{obs,1}$ with increasing [ADP] is not consistent with a one-step binding mechanism for ADP and requires a *minimum* of two steps (e.g., Scheme 2). Direct fitting of the experimental data to Scheme 2 using FITSIM yields the four rate constants in Table 1 with uncertainties of <15%. The predicted time dependence of the distribution of Rep species for the parallel binding of mantATP (3 μM) and ADP (150 μM) to Rep (0.2 μM) is shown in Figure 5C, along with the predicted (trace 6) and observed time dependencies of the total fluorescence intensity.

The major mechanistic difference between the binding of ADP and ATP is that the initial step for ADP binding is rapidly reversible on the time scale of mantATP binding, due to a much larger rate constant for dissociation of the P−ADP complex ($k_{-1,A}$). This rapid equilibration leads to a reduction in $k_{obs,1}$. The plateau value of ~14 s^{-1} (Figure 5B) is a function of both the sum of the first-order rate constants for mantATP binding ($k_{-1,M} + k_{+2,M} + k_{-2,M} \sim 6$ s^{-1}) and the rate constant for the conformational change for the P−ADP complex ($k_{+2,A} \sim 8$ s^{-1}). A smaller difference is also observed in the reverse rate constant for the second step ($k_{-2,A}$), although the estimate of this rate constant for ATP is subject to relatively large uncertainties (see earlier).

Binding of AMP and Adenosine to Rep Monomer. One advantage of the kinetic competition approach is that the equilibrium binding constants (and, in some cases, the rate constants) for the interaction of Rep with very weakly binding ligands can be determined under nonequilibrium conditions. Unlike equilibrium competition experiments, the measurements do not depend on the relative binding affinity of the labeled (either radioactively or fluorescently) nucleotide and the competing ligand (John et al., 1990). We therefore applied these methods to examine the weak binding of AMP and Ado. Kinetic competition experiments with

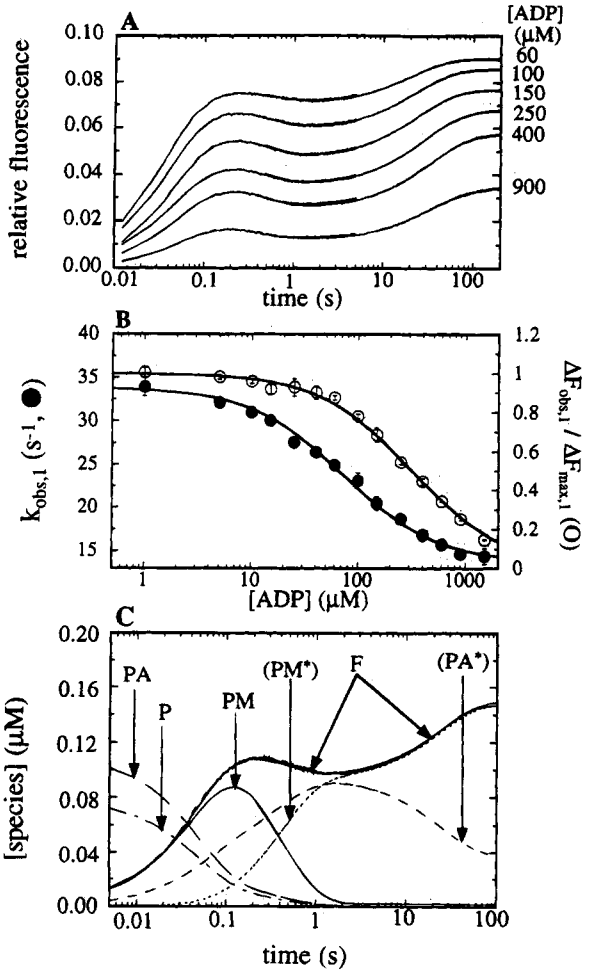

FIGURE 5: Binding of ADP to the Rep monomer in competition with mantATP. (A) Kinetic competition experiments were performed with 0.2 μM Rep and 3 μM mantATP as described in Figure 1, except that ADP was used as the competitor nucleotide. Representative traces at six [ADP] are shown. An additional series of traces (not shown) was obtained from 2 to 200 ms. (B) Dependence of $k_{obs,1}$ and $\Delta_{Fobs,1}$ on [ADP] from experiments such as those shown in A. (●) $k_{obs,1}$: Data were fit to a hyperbola with intercept = 34 (±0.4) s^{-1}, plateau = 13.6 (±0.5) s^{-1}, K_{app} = (1.39 ± 0.12) × 10^4 M^{-1}. (○) $\Delta F_{obs,1}$: Data were fit to eq 2, yielding an *apparent* association rate constant of (1.14 ± 0.04) × 10^5 M^{-1} s^{-1}. (C) KINSIM simulation of the species distribution in a kinetic competition experiment for 3 μM total mantATP and 150 μM total ADP. Rate constants for ADP are taken from Table 1, while for mantATP, $k_{+1,M}$ = 1.1 × 10^7 M^{-1} s^{-1}, $k_{-1,M}$ = 3.5 s^{-1}, $k_{+2,M}$ = 2.5 s^{-1}, and $k_{-2,M}$ = 0.034 s^{-1}.

AMP or Ado showed only two phases, where the observed rate constants for both phases, $k_{obs,1}$ and $k_{obs,2}$, decreased hyperbolically with increasing [AMP] or [Ado] (Figure 6A). The most simple interpretation of these data is that the binding of these ligands to Rep is rapidly reversible relative to the rate of mantATP binding (see the following). Under these conditions, the dependence of $k_{obs,1}$ on the concentration of the weakly binding ligand, L, is given by eq 4, where K_L is the effective equilibrium association constant for L.

$$k_{obs,1} = \{k_{+1,M}/(1 + K_L[L])\}[\text{mantATP}] + k_{-1,M} + k_{+2,M} + k_{-2,M} \quad (4)$$

From fitting the data in Figure 6A to eq 4, we obtain equilibrium association constants of (1.04 ± 0.04) × 10^4 and 93 (±4) M^{-1} for AMP and Ado, respectively. For analysis of the Ado data, the end point was fixed at 5 s^{-1} since the limited solubility of Ado precluded measurements at concentrations higher than 10 mM. The data with AMP were sufficiently well defined to allow an analysis of the entire experimental time courses using FITSIM, which yielded values of $k_{+1,A}$ = (6.9 ± 0.3) × 10^6 M^{-1} s^{-1}, $k_{1,A}$ = 680 (±30) s^{-1}, and $K_{1,A}$ = (0.99 ± 0.06) × 10^4 M^{-1} (Table 1). Due to its weak binding, the effective rate constant of dissociation of AMP from Rep could not be determined directly by mixing a Rep−AMP complex with excess mantATP. However, upon mixing a Rep−mantAMP complex (0.2 μM Rep, 100 μM mantAMP) with excess (2 mM) ATP, a rapid decrease in fluorescence intensity occurred, with an exponential rate constant of ~700 (±100) s^{-1}. The rapid dissociation of AMP and mantAMP from Rep validates the rapid equilibrium assumption inherent in the derivation of eq 4. The absence of any slower component of the fluorescence change suggests that the binding of mantAMP is likely to be a one-step reaction. A similar absence of any additional phase from the kinetic competition experiments with AMP or with Ado is also consistent with simple one-step binding of these ligands.

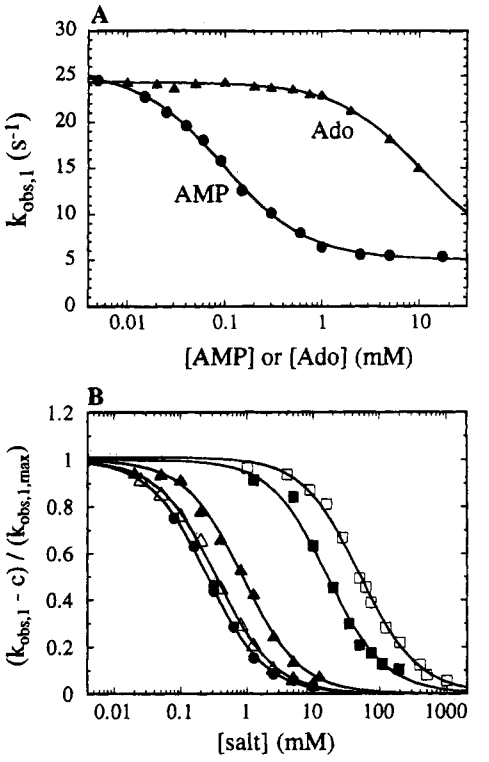

FIGURE 6: Interaction of the Rep monomer with weakly binding ligands, AMP and Ado. (A) Kinetic competition experiments were performed with 0.2 μM Rep and 2 μM mantATP as described in Figure 1 using either AMP or Ado as the competing nucleotide. The fluorescence transients are described by the sum of two exponentials defining observed rate constants $k_{obs,1}$ and $k_{obs,2}$. Dependence of $k_{obs,1}$ on [AMP] and [Ado]. The solid lines are best fits of the data to eq 4, with K_{AMP} = (1.04 ± 0.04) × 10^4 M^{-1} and K_{Ado} = 93 (±4) M^{-1}. The plateau in $k_{obs,1}$ at high [AMP] = $k_{-1,M}$ + $k_{+2,M}$ + $k_{-2,M}$ = 5.0 (±0.1) s^{-1} is equivalent to the value of c in panel B. (B) Same as for panel A, except that various salts were added to mantATP. The value of $k_{obs,1}$ is plotted on a relative scale, as described in the text. The solid lines are the best fits of the data to hyperbolae: (●) $(NH_4)_2SO_4$, K_{app} = (4.0 ± 0.2) × 10^3 M^{-1}; (△) Na_2SO_4, K_{app} = (2.9 ± 0.1) × 10^3 M^{-1}; (▲) NaP_i, K_{app} = (1.2 ± 0.1) × 10^3 M^{-1}; (■) NH_4Cl, K_{app} = 59 (±4) M^{-1}; (□) NaCl, K_{app} = 20 (±1) M^{-1}.

Effects of Salt Concentration on mantATP Binding to the Rep Monomer. Since the rate constant for the dissociation of ATP from P−ATP ($k_{-1,A}$) is small relative to the forward rate constant for the second step ($k_{+2,A}$), it is not possible to conclude unambiguously that ATP binding is a two-step process solely on the basis of the data in Figure 1. However, if experimental conditions could be obtained such that $k_{-1,A} > k_{+2,A}$ for ATP, then direct evidence for the presence of a two-step binding mechanism could be obtained from kinetic competition experiments. One possible approach would be to perform the kinetic competition experiments at higher salt concentrations, although it is first necessary to determine the salt dependencies of the rate constants in Scheme 1 for the binding of Rep to mantATP alone. Studies of the salt dependencies of the rate constants in Scheme 1 are also needed for future studies of the influence of nucleotides on the kinetics of Rep−DNA interactions and Rep-catalyzed DNA unwinding. In these studies, we examined a variety of different salts, including NaCl, NH_4Cl, Na_2SO_4, $(NH_4)_2SO_4$, and sodium phosphate, to determine whether any changes in the kinetics of mantATP binding were due to specific cation or anion effects.

Stopped-flow studies of the binding of Rep (0.2 μM) to mantATP (2 μM) were performed in buffer A, as described in the accompanying paper (Moore & Lohman, 1994). The salt concentration in these experiments was varied by adding the appropriate salt to the mantATP solution in buffer A at twice its final concentration. However, identical results were obtained when the salt concentration was increased in both the Rep and mantATP solutions. With increasing salt concentration, both observed rate constants, $k_{obs,1}$ and $k_{obs,2}$, describing the two phases of the fluorescence change, decreased hyperbolically with increasing [salt], as shown in Figure 6B. For each salt studied, the low-salt and high-salt limiting values of $k_{obs,1}$ were identical and independent of salt type, with values of 25 (±2) and 6 (±1) s^{-1}, respectively. In Figure 6B, the values of $k_{obs,1}$ were normalized to allow easier comparisons among the experiments in the different salts, where $k_{obs,1,max}$ [=25 (±2) s^{-1}] is the observed rate constant in buffer A in the absence of added salt, while c is the limiting rate constant at high [salt] [6 (±1) s^{-1})]. The dependence of $k_{obs,2}$ on [salt] and type was similar to that shown in Figure 6B.

Figure 6B indicates that the different salts show quantitatively different effects on the kinetics of mantATP binding to the Rep monomer. The midpoint salt concentrations for each curve in Figure 6B (i.e., the salt concentrations required to reduce $k_{obs,1}$ to 50% of its low-salt value) are 250 μM for $(NH_4)_2SO_4$, 340 μM for Na_2SO_4, 0.83 mM for NaP_i, 17 mM for NH_4Cl, and 50 mM for NaCl. The striking feature of the data in Figure 6B is that the sulfate and phosphate salts are much more effective inhibitors of mantATP binding than chloride salts. However, a smaller specific cation effect is also apparent upon comparing the effects of NH_4Cl and NaCl. Both of these observations indicate that the salt effects observed here do not result from simple ionic strength effects and suggest that the primary cause of the inhibition is due to specific binding of the ions to the Rep monomer (see Discussion). Although there is a 2-fold difference in the curves for NaCl *vs* NH_4Cl, indicating a specific cation effect in the 20−50 mM salt range, comparison of the curves for Na_2SO_4 and $(NH_4)_2SO_4$ indicates only a slight influence of Na^+ *vs* NH_4^+ at salt concentrations <1 mM. Therefore, in this low-salt concentration range, the primary effect of salt seems to result from divalent anion binding to Rep. Kinetically, the most simple interpretation of these data is that increasing [salt] reduces the association rate constant for mantATP ($k_{+1,M}$), with no effect on the sum of the first-order rate constants ($c = k_{-1,M} + k_{+2,M} + k_{-2,M}$). A direct test of this interpretation is described here for NaP_i and $(NH_4)_2SO_4$.

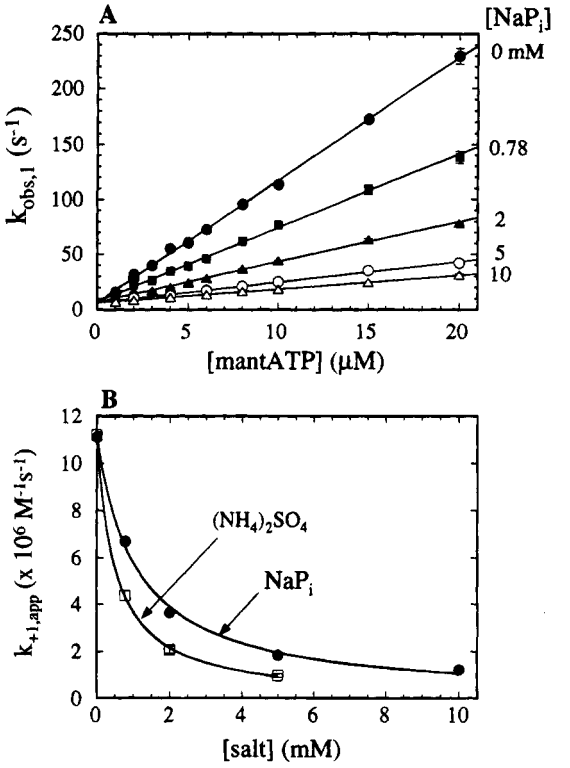

FIGURE 7: Specific ion effects on the kinetics of mantATP binding to Rep monomer. (A) Rep monomer (0.2 μM) in buffer A containing NaP_i (0−10 mM) was mixed in a stopped-flow apparatus with mantATP (1−20 μM) in buffer A containing the same concentration of NaP_i. The biphasic fluorescence change was fit to the sum of two exponentials, with observed rate constants $k_{obs,1}$ and $k_{obs,2}$. Dependence of $k_{obs,1}$ on [mantATP] at a series of [NaP_i]. The solid lines are best fits of the data to eq 4, with intercepts at 0, 0.78, 2, 5, and 10 mM NaP_i of 6.4 (±1.0), 7.2 (±1.0), 6.7 (±0.8), 6.2 (±0.6), and 6.2 (±0.3) s^{-1}, respectively. The slopes of the lines ($k_{+1,M,app}$) are shown in panel B. (B) Dependence of $k_{+1,M,app}$ on [NaP_i] and [$(NH_4)_2SO_4$]. The solid lines are the best fits of the data to eq 4, yielding $K_L = (0.93 \pm 0.13) \times 10^3$ M^{-1} for NaP_i and $(1.9 \pm 0.1) \times 10^3$ M^{-1} for $(NH_4)_2SO_4$ and $k_{+1,M} = (1.12 \pm 0.02) \times 10^7$ M^{-1} s^{-1}.

We carried out a more extensive investigation of the effects of [NaP_i] and [$(NH_4)_2SO_4$] on the kinetics of mantATP binding to Rep. As shown in Figure 7A, $k_{obs,1}$ increases linearly with [mantATP] in experiments performed at several [NaP_i]. The apparent association rate constant, $k_{+1,M,app}$, determined from the slopes of these lines, decreases hyperbolically to zero with increaing [NaP_i], as shown in Figure 7B. However, all intercepts of the lines in Figure 7A, which define the sum ($k_{-1,M} + k_{+2,M} + k_{-2,M}$), are equal and independent of [NaP_i], with a value of 6.6 (±0.6) s^{-1}. Since neither the limting value of $k_{obs,2}$ at high [mantATP] ($k_{+2,M} + k_{-2,M}$) nor the net dissociation rate constant ($k_{off} \approx k_{-2,M}$) was affected significantly by NaP_i at these concentrations (data not shown), we conclude that all three first-order rate constants are unaffected by [NaP_i] and that the primary effect of NaP_i is to reduce the apparent second-order rate constant,

k_{+1}. The results of similar experiments with $(NH_4)_2SO_4$ are shown in Figure 7B and indicate that this salt also inhibits mantATP binding primarily by reducing the apparent second-order rate constant. This inhibition presumably results from direct competitive binding of SO_4^{2-} and inorganic phosphate (HPO_4^- and/or $H_2PO_4^{2-}$) to the ATP binding site in Rep. The data with NaCl and NH_4Cl shown in Figure 6B are consistent with this interpretation, although these monovalent salts do not bind as tightly to Rep as do the divalent anions, since inhibition is observed only at much higher NaCl and NH_4Cl concentrations.

Kinetics of ATP Binding to Rep in the Absence of Mg^{2+}. Although interesting in their own right, the results presented above suggest that changes in salt concentration cannot be used to alter the rate constants for ATP dissociation from P−ATP ($k_{-1,A}$) relative to the forward rate constant for the second step ($k_{+2,A}$). However, we have shown in the accompanying paper (Moore & Lohman, 1994) that while the removal of Mg^{2+} does not appear to alter the *mechanism* of mantATP binding, it does increase $k_{-1,M}$ relative to $k_{+2,M}$. If the same effect is observed with ATP, then experiments performed in the absence of Mg^{2+}may be useful to distinguish between one- and two-step mechanisms for ATP binding to Rep.

If ATP is able to bind to Rep in the absence of Mg^{2+}, as described in Scheme 1, the dissociation of ATP from a Rep−ATP complex should display a biphasic fluorescence change [e.g., see Figure 8C of Moore and Lohman (1994)], whereas a single-exponential decay would be observed for a one-step binding mechanism. Figure 8A shows that a clear biphasic time course is observed when 0.2 μM Rep plus 20 μM ATP was mixed with 200 μM mantATP. The fast phase of the fluorescence change, with $k_{obs,1} \sim 440$ (±25) s^{-1} ($\Delta F_1 \sim 0.7$), probably corresponds to rapid dissociation of ATP from P−ATP, while the slower phase with $k_{obs,2} \sim 28$ (±1) s^{-1} ($\Delta F_2 \sim 0.3$) reflects the net off-rate of ATP dissociation from (P−ATP)*. These values of $k_{obs,1}$ and $k_{obs,2}$ are similar to those observed for the biphasic dissociation of mantATP from Rep under identical conditions (240 and 29 s^{-1}, respectively). These data provide strong evidence for the presence of two distinct Rep−ATP complexes that occur at equilibrium in the absence of Mg^{2+}.

Direct evidence for a two-step binding mechanism for ATP under these conditions also comes from a series of kinetic competition experiments performed with 5 μM mantATP and varying [ATP] (0−50 μM) in the absence of Mg^{2+} (Figure 8B). From the equilibrium fluorescence intensities at each [ATP] and the knowledge that $K_{mantATP} = 0.53$ (±0.04) μM^{-1} (Moore & Lohman, 1994), we calculate $K_{ATP} = 0.27$ (±0.03) μM^{-1} from eq 3. If ATP binds to Rep via a one-step mechanism, then a value of $k_{-1,A} = 28$ s^{-1} (see Figure 8A) would require that $k_{+1,A} = 7.6 \times 10^6$ M^{-1} s^{-1}. In Figure 8C we show the experimental data obtained at 20 μM ATP (from Figure 8B), along with a simulated fluorescence transient (curve b) based on the known rate constants for mantATP binding (Moore & Lohman, 1994) and the apparent values of $k_{+1,A}$ and $k_{-1,A}$ calculated from the assumption of one-step binding of ATP. Clearly, the assumption of one-step binding is inconsistent with the experimental results, and thus we conclude that a two-step binding mechanism must apply for ATP in the absence of Mg^{2+}. Figure 8C also shows that a simulated time course (curve a) based on Scheme 2, with $k_{+1,A} = 9 \times 10^7$ M^{-1} s^{-1}, $k_{-1,A} = 440$ s^{-1}, $k_{+2,A} = 10$ s^{-1}, and $k_{-2,A} = 28$ s^{-1}, superimposes on the experimental time course. These rate constants, obtained by iterative fitting of the data in Figure 8A,B using KINSIM, provide a good description of the experimental data and are very similar to those obtained for mantATP binding under identical conditions (Moore & Lohman, 1994).

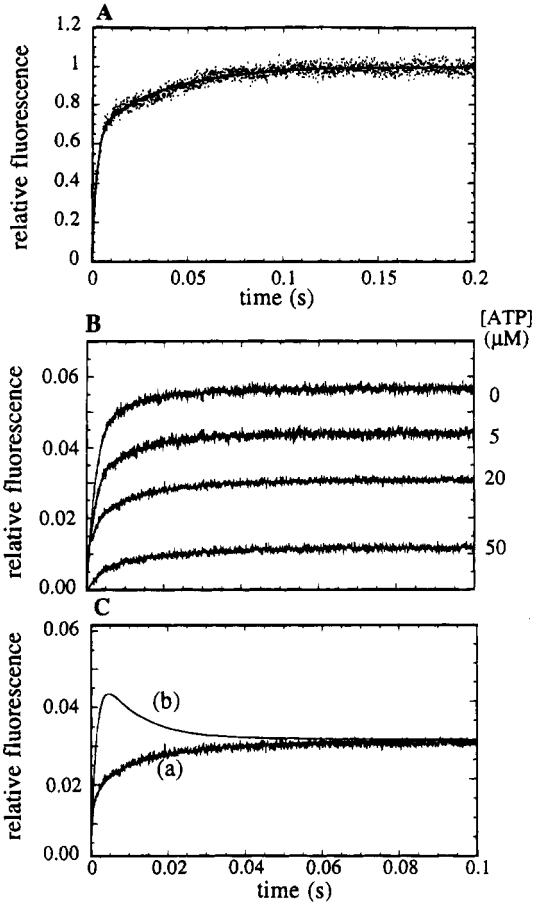

FIGURE 8: Two-step binding and dissociation of ATP from Rep monomer in the absence of Mg^{2+}. (A) Rep monomer (0.2 μM) plus ATP (20 μM) in 20 mM Tris·HCl (pH 7.5), 6 mM NaCl, 2 mM EDTA, and 10% (v/v) glycerol (buffer AE) was mixed in a stopped-flow experiment with mantATP (200 μM) in the same buffer at 4 °C. The solid line is the best fit of the data to a double-exponential function, with observed rate constants of 440 (±25) and 28 (±1) s^{-1} ($A_1 = 0.65$ (±0.05) and $A_2 = 0.35$ (±0.05)). (B) Rep monomer (0.2 μM) in buffer AE was mixed in a stopped-flow apparatus with a solution of mantATP (5 μM) plus ATP (0−50 μM) in the same buffer at 4 °C. Four representative experiments are shown. From the equilibrium fluorescence intensity at each [ATP], we calculate $K_{ATP} = 0.27$ (±0.04) s^{-1} (eq 3). (C) The experiment from panel B obtained at 20 μM ATP is shown with two simulated curves (curve a superimposes over the data). Curve a is derived from Scheme 2, with $k_{+1,M} = 8 \times 10^7$ M^{-1} s^{-1}, $k_{-1,M} = 240$ s^{-1}, $k_{+2,M} = 30$ s^{-1}, and $k_{-2,M} = 40$ s^{-1} [taken from Moore and Lohman (1994), accompanying paper] and $k_{+1,A} = 9 \times 10^7$ M^{-1} s^{-1}, $k_{-1,A} = 440$ s^{-1}, $k_{+2,A} = 10$ s^{-1}, and $k_{-2,A} = 28$ s^{-1}. Curve b is simulated assuming the binding of ATP is a one-step process, with $k_{+1,A} = 7.6 \times 10^6$ M^{-1} s^{-1}, $k_{-1,A} = 28$ s^{-1}, and $k_{+2,A} = k_{-2,A} = 0$.

DISCUSSION

Kinetic Competition Approach to Monitor Ligand Binding to Rep and Other Helicases. We have used kinetic competition experiments with the fluorescent nucleotide analogue, mantATP, to investigate the mechanism of Rep monomer binding to ATP, ADP, ATPγS, AMPPNP, and other non-fluorescent nucleotides. Kinetic competition experiments

have been used to study several nucleotide binding proteins either where binding occurs by a simple one-step reaction (Eccleston & Trentham, 1979; Novak & Goody, 1988) or where the initial association steps in Scheme 2 were assumed to be in rapid equilibria (Bagshaw & Trentham, 1974; John et al., 1990). In these cases, analytical approximations for the concentration dependence of the observed rate constants can be obtained. The results presented here and in the accompanying paper (Moore & Lohman, 1994) are consistent with two-step binding mechanisms for both mantATP and the parent nucleotides (ATP, ADP, etc.); however, the first step is not in rapid equilibrium. Under these circumstances, rate expressions for Schemes 2 and 3 cannot be obtained in closed-form, and analysis of the kinetic competition data requires the use of iterative computer fitting routines such as FITSIM (Barshop et al., 1983; Zimmerle et al., 1987; Zimmerle & Frieden, 1989). The use of FITSIM also allows one to incorporate amplitude information in the fitting process, and this latter feature has proven to be essential for the analysis of the experiments described here.

The kinetic competition studies described here extend our mechanistic conclusions that were based on mant nucleotide binding to the *E. coli* Rep monomer [Moore and Lohman (1994), accompanying paper]. A primary objective was to determine whether the two-step mechanism proposed for the binding of mant nucleotides is also applicable to the corresponding unmodified nucleotides and to determine the kinetic rate constants for ATP and ADP binding under the solution conditions used in our DNA binding studies (Wong et al., 1992; Wong & Lohman, 1992). These stopped-flow studies represent the first characterization of the kinetic mechanism of nucleotide binding to a helicase. We have also used this approach to quantitatively monitor the interaction of Rep monomer with AMP, Ado, inorganic phosphate, and SO_4^{2-}, ligands that bind too weakly to permit an accurate estimation of the binding affinity by many equilibrium techniques. The approaches described here and in the accompanying paper (Moore & Lohman, 1994) are generally applicable to the study of nucleotide binding to the functional Rep dimer helicase that forms upon binding DNA (Chao & Lohman, 1991), as well as to other helicases. Furthermore, the kinetic competition approach could be applied equally well to the study of DNA binding kinetics using fluorescently labeled DNA substrates.

Kinetic Mechanism of ATP Binding to the Rep Monomer. Our studies of ATP binding to Rep in the presence of 5 mM Mg^{2+} could not be used to distinguish unambiguously between mechanisms requiring one *vs* two steps, and attempts to resolve this ambiguity by changing the salt concentration and thus the relative rate constants were unsuccessful. Nevertheless, we propose that ATP binds in a two-step mechanism by analogy with all of the other nucleotides studied (except AMP, mantAMP, and Ado; see below), and since Scheme 2 represents the minimum mechanism needed to describe the kinetic competition data for the binding of ATP to Rep in the absence of Mg^{2+}. The ambiguity that arises between one- and two-step mechanisms for the binding of ATP in the presence of 5 mM Mg^{2+} is a kinetic consequence of the slow dissociation of ATP from the initial collisional complex relative to the rate of the conformational change.

The sequential two-step binding mechanism shown in Scheme 1 is often difficult to distinguish kinetically from a

Scheme 4

$$\text{P–mantATP} \underset{k_{-1,M'}}{\overset{k_{+1,M'}}{\rightleftharpoons}} \text{P} + \text{mantATP} \underset{k_{-2,M'}}{\overset{k_{+2,M'}}{\rightleftharpoons}} (\text{P–mantATP})^*$$

mechanism involving two distinct binding modes for the nucleotide (Scheme 4) [see Bagshaw et al. (1974) and Viale (1971)]. However, analysis of the kinetic competition data with ADP and AMPPNP by Scheme 4 would require values of $k_{+2,A'} = 1.4 \times 10^5$ and $\sim 5 \times 10^5$ M^{-1} s^{-1} for ADP and AMPPNP, respectively. However, these rate constants are 2−3 orders of magnitude lower than typical protein−ligand association rate constants (10^7−10^8 M^{-1} s^{-1}; Gutfreund, 1972; Fersht, 1985), and binding would therefore be uncharacteristically slow. For this reason, we prefer Scheme 1 rather than Scheme 4 to describe the biphasic kinetics of nucleotide binding to the Rep monomer.

In the accompanying paper (Moore & Lohman, 1994), we show that the removal of Mg^{2+} from Rep dramatically alters the kinetics of mantATP association and dissociation. Quantitatively similar results were obtained with ATP, and importantly, a *minimum* of two steps in the binding mechanism was required to describe the data. The rate and equilibrium constants for ATP are within a factor of 2−3 of those observed with mantATP, indicating that the binding of mantATP observed in the absence of Mg^{2+} is not due to specific interactions of the fluorophore with the protein. The possible significance of these results to the mechanism of nucleotide binding by Rep has been discussed previously in the context of mantATP binding (Moore & Lohman, 1994) and also appears to be valid for ATP.

Kinetic Mechanisms of ATPγS and AMPPNP Binding to the Rep Monomer. As we have described for the corresponding mant derivatives (Moore & Lohman, 1994), ATPγS is a better kinetic analogue of ATP than is AMPPNP. Whereas relatively minor changes in the rate and equilibrium constants were observed upon thio substitution, the kinetic mechanism of AMPPNP binding differs qualitatively and quantitatively from that observed with ATP. The kinetic competition studies with AMPPNP described here confirm and extend our observations with mantAMPPNP. The initial binding step was shown to be a rapid equilibrium, and direct evidence for a third complex, (P−AMPPNP)**, was obtained. A similar three-step binding mechanism is also required on the basis of the results of kinetic competition experiments, using 3′-mant-dATP as the fluorescent nucleotide (data not shown), where the rate constants were very similar to those given in Table 2. While AMPPNP is often described as a slowly binding ATP analogue, with Rep the initial association rate constant ($k_{+1,A}$) is, in fact, identical to that observed with ATP; AMPPNP binding only appears macroscopically slow due to the rapid dissociation of AMPPNP from the collisional complex.

The significance of the additional binding step with AMPPNP is not immediately obvious in the absence of structural information. Different interpretations can be formed, depending on whether the same (or an analogous) end conformation is assumed to form with both ATP and AMPPNP. The observation that the dissociation rate constant of AMPPNP from (P−AMPPNP)** is similar to that of ATP from (P−ATP)* suggests this possibility. The fact that the initial binding steps for ADP and AMPPNP (and in fact AMP; see below) are similar suggests that interactions

of Rep with ATP, which result in slow dissociation from P−ATP, do not form in the initial collisional complex with AMPPNP (or ADP or AMP). If so, a rearrangement of P−AMPPNP would then be required to achieve the conformation (P−AMPPNP)*, which may be analogous to P−ATP. Regardless of the interpretation, the data clearly indicate that substitution of the bridging oxygen in ATP for an imido linkage dramatically alters the kinetics and equilibrium binding of Rep with the nucleotide. We note, however, that the use of mantAMPPNP in kinetic competition studies with the Rep dimer species may be useful when the binding of mantATP or mantATPγS is too rapid to measure accurately or when the hydrolysis of mantATPγS or ATPγS is significant over the time course of the experiments. For the latter reason, AMPPNP was used in our equilibrium studies of the effects of nucleotides on DNA binding to Rep (Wong & Lohman, 1992).

Kinetic Mechanism of ADP, AMP, and Adenosine Binding to the Rep Monomer. The results of kinetic competition studies with ADP are significant in that they exclude a one-step mechanism for the binding of this nucleotide to Rep, even in the presence of 5 mM Mg^{2+}. A similar conclusion is reached on the basis of experiments performed with 3′-mant-dATP as the fluorescent nucleotide (data not shown), where $k_{obs,1}$ decreases with increasing [ADP] and reaches a plateau at $\approx$13 s^{-1}. This gives further support to a two-step mechanism for ATP binding to Rep, since we are not aware of a system where two-step binding is observed for ADP (GDP) but not for ATP (GTP) [for examples, see Moore and Lohman (1994) accompanying paper). In general, the equilibrium association constant for the first step (K_1) is reduced with ADP (GDP) relative to ATP (GTP), whereas the forward rate for the unimolecular second step is comparable for both nucleotides. It has been suggested (Bagshaw et al., 1974) that this change in K_1 generally reflects an increase in k_{-1} for ADP (GDP); this is the case for the Rep monomer, as we show here.

The terminal phosphate of ATP clearly is important for interactions with Rep, since $k_{-1,A}$ is so much lower for ATP than for ADP or AMP. It is interesting to note that the removal of Mg^{2+} increases $k_{-1,A}$ for ATP to a value that is comparable to that observed with ADP or AMP in the presence of Mg^{2+}. Since $k_{-1,A}$ and $k_{+1,A}$ are the same for ADP and AMP, this suggests that the initial recognition of nucleotide by Rep is unaffected by the presence or absence of the β-phosphate of ADP. The lower equilibrium constant for AMP *vs* ADP binding to Rep can be correlated with the absence of the second step from the binding of AMP, suggesting that the importance of the β-phosphate for tight binding is reflected in steps that occur subsequent to the formation of the initial collisional complex. A similar suggestion was made for the binding of guanine nucleotides and nucleosides by $p21^{ras}$ (John et al., 1990), where the second step in the binding mechanism with GTP and GDP was proposed to be associated with changes in the structure of the phosphate binding loop. The dramatic change in nucleotide binding kinetics that we observe upon the removal of Mg^{2+} is consistent with this interpretation for Rep.

There appears to be a linear relationship between the apparent equilibrium association constant and the number of phosphate groups in the nucleotide, since the removal of each of the α-, β-, and γ-phosphates from ATP is associated with a 100-fold reduction in the overall binding constant. As discussed earlier, the mechanistic reasons for these macroscopic differences vary for each nucleotide. However, the relatively weak binding of Ado to Rep ($K_a \approx 10^2$ M^{-1}) clearly indicates the important energetic contributions to binding made by the phosphate groups. Consistent with this idea, Rep binds to other ribonucleoside triphosphates with only 30−100-fold lower affinities than it does to ATP (Arai et al., 1981).

Using nitrocellulose filter binding, Arai et al. (1981) studied the equilibrium binding of nucleotides to the Rep monomer (in the absence of DNA) under comparable experimental conditions (20 mM Tris·HCl (pH 7.5, 0 °C), 8 mM $MgCl_2$, 0.1 mM dithiothreitol, 0.1 mg/mL bovine serum albumin, and 10% (v/v) glycerol). Although the relative binding affinities of ATP, ADP, AMPPNP, and ATPγS reported by Arai et al. (1981) are qualitatively consistent with our results, the equilibrium association constants that we determine are 5−10-fold higher.

Ion-Specific Effects on the Binding of Adenine Nucleotides to the Rep Monomer. Using a variety of different salts, we have found that increasing [salt] inhibits mantATP binding to the Rep monomer. However, these effects of salt (Figures 6B and 7) cannot be explained solely in terms of Debye−Huckel-type screening (ionic strength) effects, since comparisons among the different salts clearly indicate the presence of ion-specific effects that must result from specific ion binding to the Rep protein. At a given salt concentration, the largest effects are observed with sulfate and phosphate salts; however, the nonequivalence of NaCl *vs* NH_4Cl also indicates that specific cation binding occurs as well. The observation of such specific ion effects in this system is not surprising since such effects are observed in most protein systems that are examined in detail [for a review, see Record et al. (1978)].

The inhibition of mantATP binding by salt appears to result primarily from a reduction in the apparent association rate constant, $k_{+1,M}$, whereas the three first-order rate constants in the mechanism, including $k_{-1,M}$, are relatively insensitive to [salt] over the range studied. The *primary* effect of salt appears to be due to an effect of the anion (cf. Cl^- *vs* SO_4^{2-}). In the case of sulfate and phosphate anions, the reduction in $k_{obs,1}$ is almost certainly due to competition between mantATP and these anions for the ATPase site [see Bagshaw and Trentham (1974)]. According to this interpretation, sulfate would act as a phosphate analogue. The dependence of $k_{obs,1}$ on [salt] would then be given by eq 4 (where L represents sulfate or phosphate). From the data in Figure 6B, we estimate $K_L \sim (3-4) \times 10^3$ M^{-1} for sulfate (depending on the cation) and $\approx 10^3$ M^{-1} for sodium phosphate. The data in Figure 7 are also consistent with the predictions of eq 4, from which we can obtain independent estimates of K_L [$(1.9 \pm 0.1) \times 10^3$ M^{-1} for sulfate and $(0.93 \pm 0.13) \times 10^3$ M^{-1} for phosphate]. The fact that $k_{+1,app}$ approaches zero at high [L] indicates that the binding of mantATP and sulfate/phosphate is mutually exclusive.

It is possible that Rep binds HPO_4^{2-} (of which SO_4^{2-} would be an analogue), and therefore at pH 7.5 the true value of K_L for HPO_4^{2-} would be $> 10^3$ M^{-1}. Interestingly, sulfate and phosphate anions bind to Rep with higher affinity than adenosine, consistent with the idea that electrostatic effects dominate the interactions between Rep and ATP and ADP. The apparent affinity of Rep for pyrophosphate ($K_L \approx 1.1$

$\times 10^3$ M^{-1}) was not significantly higher than that for P_i (data not shown).

The mechanism by which NaCl and NH_4Cl reduce the apparent rate constant for mantATP binding to Rep is less clear. Since the inhibition of mantATP binding by these salts has the same form as that observed with sulfate and phosphate (Figure 6B), Cl^- could, in principle, reduce $k_{+1,M,app}$ by competing with mantATP for binding, albeit with ~100-fold lower affinity than sulfate and phosphate. However, specific cation effects (Na^+ *vs* NH_4^+) are also apparent and must reflect the presence of specific cation binding sites on the Rep protein.

Previous studies of the two-step binding of ATP to myosin over a range of KCl concentrations similar to those used here with NaCl and NH_4Cl were interpreted as an effect due to changes in ionic strength (Bagshaw et al., 1974; Johnson & Taylor, 1978), although this was not tested directly. Since the form of the inhibition predicted from an ionic strength effect (see Figure 5; Johnson & Taylor, 1978) is very similar to the hyperbolic decrease in the apparent association rate constant predicted by eq 4 (see Figure 6B), it is essential to compare results with several salt types in order to differentiate ionic strength effects from those due to direct ion binding to the protein (Record et al., 1978; Lohman, 1986). In fact, the linear increase in the maximal rate of the fluorescence change (k_{+2} in Scheme 1) with increasing [KCl] observed by Johnson and Taylor (1978) suggests specific ion binding by the myosin−ATP complex.

Comparison with Equilibrium Binding Studies of Nucleotide to Other Helicases. On the basis of the studies reported here and in the accompanying paper (Moore & Lohman, 1994), we write the following scheme in which the two-step binding mechanisms for ATP (T) and ADP (D) are linked by the DNA-independent ATPase activity of the Rep monomer (4 °C, pH 7.5, 10% (v/v) glycerol, 6 mM NaCl, and 5 mM $MgCl_2$):

$$P + T \underset{1.5\ s^{-1}}{\overset{1.2 \times 10^7\ M^{-1}\ s^{-1}}{\rightleftharpoons}} PT \underset{0.9\ s^{-1}}{\overset{15\ s^{-1}}{\rightleftharpoons}} PT^* \xrightarrow{0.002\ s^{-1}}$$

$$PD^* \underset{8\ s^{-1}}{\overset{0.067\ s^{-1}}{\rightleftharpoons}} PD \underset{6.7 \times 10^6\ M^{-1}\ s^{-1}}{\overset{720\ s^{-1}}{\rightleftharpoons}} P + D$$

The only information that is missing from this scheme is the rate constant for phosphate release from the Rep−ADP−P_i complex. However, the absence of a burst in product formation in multiple-turnover experiments suggests that P_i release occurs at >0.002 s^{-1}. Under these conditions, ATP binding to the Rep monomer is tighter than that of ADP, primarily as a result of differences in k_{-1}.

It is of interest to compare our results with the information available on nucleotide binding to other helicases. However, in so doing, we reemphasize that the results reported here are for the Rep monomer, whereas DNA binding induces Rep to dimerize and form the functionally active form of the helicase (Chao & Lohman, 1991). In fact, DNA binding stimulates the intrinsic ATPase activity of the Rep monomer by 10^3−10^4-fold, depending on the type of DNA used (double-stranded (ds) *vs* single-stranded (ss)) (Wong et al., 1993; K.J.M.M., unpublished experiments). Whereas no detailed kinetic studies of nucleotide binding to other helicases have been reported, equilibrium binding of adenine nucleotides has been studied for the *E. coli* rho and the *E. coli* DnaB proteins in the absence of nucleic acids. The *E. coli* rho protein has a DNA:RNA helicase activity that has been implicated in the release of nascent RNA transcripts from transcription complexes paused at rho-dependent termination sites (Brennan et al., 1987), and the *E. coli* DnaB protein is an ATP-dependent DNA helicase that functions in both the initiation and elongation stages of DNA replication (Kornberg & Baker, 1992). In contrast to Rep, both the DnaB and rho helicases appear to function as hexamers, which can form in the absence of nucleic acid. In general, the affinity of Rep monomer for nucleotides that we observe is 1 or 2 orders of magnitude higher than is observed with the hexameric rho and DnaB helicases (see below).

The hexameric rho helicase possesses two classes of ATP binding sites that differ by ~30-fold in affinity (Geiselmann & von Hippel, 1992). A rho monomer or dimer retains the ability to bind ATP, with the monomeric form having a relatively higher affinity for nucleotide (Geiselmann & von Hippel, 1992). Rep is similar to rho in this regard since a Rep dimer (bound to either ss- or ds-DNA) has a lower affinity for ATP than does the monomer (K.J.M.M. and T.M.L., unpublished results). Stitt (1988) reported that ATP binds to the tight site on a rho hexamer with ~100-fold higher affinity than either ADP or AMPPNP. Similar results are obtained with the Rep monomer, as shown here and previously (Arai et al., 1981). The kinetic basis for these differences that we find with Rep may also be applicable to rho. However, both inorganic phosphate and AMP bind more weakly to rho ($K_{P_i} \approx 30$ M^{-1}, $K_{AMP} \ll 10^3$ M^{-1}; Stitt, 1988) than to Rep ($K_{P_i} \approx 10^3$ M^{-1}, $K_{AMP} \approx 10^4$ M^{-1}; Table 1). Nucleotide binding to rho was not detectable in the absence of Mg^{2+} using spin column methods (Stitt, 1988), whereas we show that nucleotides do bind to Rep in the absence of Mg^{2+} (although with significantly different kinetics). However, as discussed in the accompanying paper (Moore & Lohman, 1994), the inability to detect nucleotide binding to rho using spin columns likely reflects the higher dissociation rate constant for nucleotide from rho in the absence of Mg^{2+}. Similarly, nucleotide binding to Rep (Arai et al., 1981) and DnaB (Arai & Kornberg, 1981; see the following) was not detectable in the absence of Mg^{2+} using nitrocellulose filter binding.

Equilibrium binding of nucleotides to the hexameric DnaB helicase has also been studied (Biswas et al., 1986; Arai & Kornberg, 1981; Bujalowski & Klonowska, 1993). As with Rep and rho, each monomer of DnaB has one site for nucleotide binding (Arai & Kornberg, 1981; Bujalowski & Klonowska, 1993). Furthermore, as with rho, three high-affinity and three low-affinity nucleotide binding sites have been reported, although this has been interpreted in terms of a negative cooperativity for nucleotide binding in the case of DnaB (Bujalowski & Klonowska, 1993). However, one major difference between DnaB and either Rep or rho is that the affinity of DnaB for ADP appears to be comparable to, or slightly higher than, that of ATP (Arai & Kornberg, 1981; Biswas et al., 1986; Bujalowski & Klonowska, 1993), whereas ATP binds ~100-fold more tightly than ADP to both Rep and rho. On the other hand, the 100-fold lower affinity of DnaB for AMP relative to ADP (Bujalowski & Klonowska, 1993) is comparable to the difference observed with Rep (Table 1). For Rep, this difference is almost entirely due to the absence of the conformational change in the kinetic mechanism of AMP binding. For all three proteins (Rep, rho, and DnaB), the affinity for AMPPNP is >100-fold lower than that for ATP, suggesting that the

mechanistic basis for this effect may be similar for each helicase.

In summary, we show that the two-step binding reaction observed with mantATP (Moore & Lohman, 1994) is an intrinsic property of nucleotide binding to the Rep monomer. Furthermore, the rate and equilibrium constants observed for mant nucleotides are comparable to those observed with the parent adenine nucleotides. This mechanism shows many similarities (and a number of significant differences) with those of other ATPases and GTPases involved in signal transduction and molecular motion. The approaches described here and in the accompanying paper (Moore & Lohman, 1994) should prove useful in future kinetic studies of the DNA-stimulated ATPase and DNA unwinding activity of the Rep dimer helicase, as well as other helicases.

ACKNOWLEDGMENT

We are indebted to Neil Millar (Kings College, London) for supplying the data simulation program KISM and to Carl Frieden (Washington University) for supplying the data simulation and fitting programs KINSIM and FITSIM. We also thank Bill van Zante for technical assistance and Isaac Wong for the Pascal program "ATOB-4K" used in the analysis of stopped-flow data by FITSIM.

REFERENCES

Amaratunga, M., & Lohman, T. M. (1993) *Biochemistry 32*, 6815−6820.

Arai, K., & Kornberg, A. (1981) *J. Biol. Chem. 256*, 5260−5266.

Arai, N., Arai, K. I., & Kornberg, A. (1981) *J. Biol. Chem. 256*, 5287−5293.

Bagshaw, C. R., & Trentham, D. R. (1974) *Biochem. J. 141*, 331−349.

Bagshaw, C. R., Eccleston, J. F., Ekstein, F., Goody, R. S., Gutfreund, H., & Trentham, D. R. (1974) *Biochem. J. 141*, 351−364.

Barshop, B. A., Wrenn, R. F., & Frieden, C. (1983) *Anal. Biochem. 130*, 134−145.

Biswas, E. E., Biswas, S. B., & Bishop, J. E. (1986) *Biochemistry 25*, 7368−7374.

Brennan, C. A., Dombroski, A. J., & Platt, T. (1987) *Cell 48*, 945−952.

Bujalowski, W., & Klonowska, M. M. (1993) *Biochemistry 32*, 5888−5900.

Chao, K., & Lohman, T. M. (1990) *J. Biol. Chem. 265*, 1067−1076.

Chao, K., & Lohman, T. M. (1991) *J. Mol. Biol. 221*, 1165−1181.

Eccleston, J. F., & Trentham, D. R. (1979) *Biochemistry 18*, 2896−2904.

Fersht, A. R. (1985) in *Enzyme Structure and Mechanism*, Freeman, San Francisco.

Geeves, M. A. (1992) *Philos. Trans. R. Soc. London B 336*, 63−71.

Geiselmann, J., & von Hippel, P. H. (1992) *Protein Sci. 7*, 850−860.

Gutfreund, H. (1972) in *Enzymes: Physical Principles*, Wiley (Interscience), New York.

Hiratsuka, T. (1983) *Biochim. Biophys. Acta 742*, 496−508.

Jackson, A. P., & Bagshaw, C. R. (1988a) *Biochem. J. 251*, 515−526.

Jackson, A. P., & Bagshaw, C. R. (1988b) *Biochem. J. 251*, 527−540.

John, J., Sohmen, R., Feuerstein, J., Linke, R., Wittinghofer, A., & Goody, R. S. (1990) *Biochemistry 29*, 6058−6065.

Johnson, K. A. (1992) in *The Enzymes*, pp 1−61, Academic Press, Inc., New York.

Johnson, K. A., & Taylor, E. W. (1978) *Biochemistry 17*, 3432−3442.

Kornberg, A., & Baker, T. A. (1992) *DNA Replication*, Freeman, San Francisco.

Lohman, T. M. (1986) *CRC Crit. Rev. Biochem. 19*, 191−245.

Lohman, T. M. (1992) *Mol. Microbiol. 6*, 5−14.

Lohman, T. M. (1993) *J. Biol. Chem. 268*, 2269−2272.

Matson, S. W. (1991) *Prog. Nucleic Acid Res. 40*, 289−326.

Matson, S. W., & Kaiser-Rogers, K. A. (1990) *Annu. Rev. Biochem. 59*, 289−329.

Moore, K. J. M., & Lohman, T. M. (1994) *Biochemistry 33*, 14550−14564.

Novak, E., & Goody, R. S. (1988) *Biochemistry 27*, 8613−8617.

Record, M. T., Jr., Anderson, C. F., & Lohman, T. M. (1978) *Q. Rev. Biophys. 11*, 103−178.

Stitt, B. L. (1988) *J. Biol. Chem. 263*, 11130−11137.

Viale, R. O. (1971) *J. Theor. Biol. 31*, 501−507.

Wong, I., & Lohman, T. M. (1992) *Science 256*, 350−355.

Wong, I., Chao, K. L., Bujalowski, W., & Lohman, T. M. (1992) *J. Biol. Chem. 267*, 7596−7610.

Wong, I., Amaratunga, M., & Lohman, T. M. (1993) *J. Biol. Chem. 268*, 20386−20391.

Woodward, S. K. A., Eccleston, J. F., & Geeves, M. A. (1991) *Biochemistry 30*, 422−430.

Zimmerle, C. T., & Frieden, C. (1989) *Biochem. J. 258*, 381−387.

Zimmerle, C. T., Patane, K., & Frieden, C. T. (1987) *Biochemistry 26*, 6545−6552.